SF2A 2011
G. Alecian, K. Belkacem, R. Samadi and D. Valls-Gabaud (eds)

GHOSTS IN SATURN'S RINGS

K. Baillié[1], J.E. Colwell[1] and L.W. Esposito[2]

Abstract. Using UVIS stellar occultation data, we identified holes in ringlets or plateaus through which we directly observed the star. These "ghosts" are characterized by an isolated peak in photon counts with a height equal to photon counts in places without ring material. We suggest that ghosts are the signatures of ephemeral structures in the rings that could be due to particularly large clumps of material or small moonlets. The usual S-shape around a "propeller" moonlet coincides with the presence of a depletion zone around the clump: these moonlets are probably not massive enough to open full gaps, but could produce azimuthally limited holes in the rings like those seen in the UVIS occultation data. Numerical simulations of the interaction of a moonlet with ring particles have been conducted for different sizes of moonlets and particles, making it possible to extrapolate a relation between the radial extension of the depletion zone and the moonlet Hill radius. This model and our observed ghost widths allowed us to estimate an initial boulder size distribution following a power-law with a cumulative index Q=0.6 – 0.8. This boulder size distribution appears not to match the particle size distribution models from Zebker et al., 1985 (Q=1.75 in the Cassini Division). Objects up to 15 m were found in the C ring and up to 60 meters in the Cassini Division.

Keywords: saturn, rings, ghosts, boulders, moonlets

1 Observations

We analyze star occultations presenting significant background photon counts (usually higher that 20 photons per integration period). The resolution of our data is of the order of 1 ms, which corresponds to about 1 to 10 m, depending on the geometry of the occultations. We focus on regions of relatively high optical depth such as the C ring and Cassini Division ringlets and we avoid regions presenting local disturbances from known waves or structures. Ghosts behave like holes in a ringlet or plateau through which we directly observe a star: it is therefore characterized by an isolated peak in photon counts with a height equal to the star photon counts in places without ring material (Figure 1). Figure 2 presents the cumulative distribution of these widths in terms of number of data points.

Statistical arguments show that the actual number of our ghosts being cosmic rays should be negligible and we can state with a good confidence that our observed ghosts that are one data point wide are actual structures in the rings.

2 Forming Ghosts: the Propeller Model

In order to understand the interactions between a moonlet and the ring particles, we evaluate the radius of the Hill sphere of a given moonlet of mass $M_{moonlet}$ and of semi-major axis $a_{moonlet}$: $r_H = a_{moonlet}\left(\frac{M_{moonlet}}{3(M_{Saturn}+M_{moonlet})}\right)^{1/3}$, where M_{Saturn} is Saturn's mass. The Hill sphere of a moonlet is the region in which its attraction dominates Saturn's attraction.

Numerical simulations of the interactions between ring particles and a moonlet showed the apparition of a depletion in surface mass density in the neighborhood of the moonlets (Petit & Henon 1988). The chaotic depletion zone where particles are cleared out by the moonlet presents two different lobes due to Keplerian

[1] Department of Physics, University of Central Florida, Orlando, Florida 32816-2385, USA
[2] Laboratory for Atmospheric and Space Physics, University of Colorado at Boulder, 392 UCB, Boulder, Colorado 80309-0392, USA

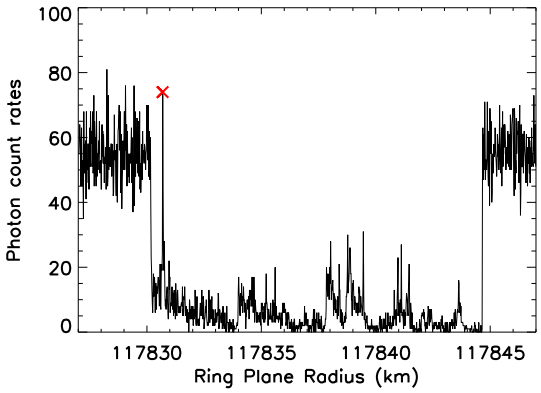

Figure 1. Photon count rates in the Huygens ringlet from the occultation of α Arae, rev. 63. The red cross identifies the position of the detected ghost. Its height matches the background level of the star.

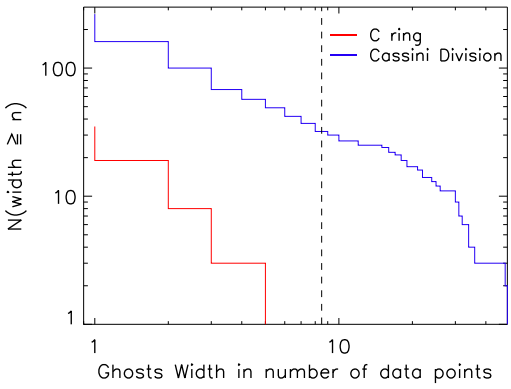

Figure 2. Cumulative width distribution of the detected ghosts in number of data points. The zone at the left of the vertical dashed line delimits the structures that we consider as ghosts with a high confidence.

shear: the inner one is carried forward while the outer one is trailing behind. Spahn & Wiebicke (1989) and Spahn et al. (1992) showed that smaller moonlets will only create localized S-shaped density modulations which radial width scales as r_H for moonlet diameters lower than 3 km and as r_H^2 for larger moonlets (Petit & Henon 1988). Moonlets larger than 2 km in diameter can lead to the formation of complete circumferential structures: diffusion is not strong enough to close the depletion before/after the moonlet, stretching it around the entire ring system. The depletion becomes a gap although the wakes are still visible close to the moonlet. Even larger moonlets (larger than 5 km in diameter) can lead to the formation of an inner ringlet, flanked by gaps. Beyond these gaps, satellite wakes are formed as described in Showalter et al. (1986). Sremčević et al. (2002) estimated that it requires a moonlet with a radius larger than 840 m to open a gap in the B ring. The S-shape of this density modulation is called a "propeller". Lewis & Stewart (2009) determined from numerical simulations that propellers can form only if the mass of the moonlet is at least 30 times higher than the mass of the largest particle in the nearby ring. Indeed, for bigger particles, self-gravity tends to accelerate the damping of the propeller-shaped gaps and prevent the formation of moonlet wakes.

Particles in close-encounters are perturbed and receive a kick in eccentricity proportional to $1/(\Delta a)^2$. In addition, the phases of these particles' orbits are roughly aligned (Showalter & Burns 1982). These now eccentric particles will leave an open space on the outer trailing side and inner leading side of the moonlet. This primary depletion zone has a radial extension of a few Hill radii while its azimuthal extension can be much larger as confirmed in numerical simulations (Figure 3). After a few orbits, the oldest and farthest depletion zones are destroyed by the combined effects of collisions and inter-particle gravitational forces provoking either a damping of the eccentricity, a randomizing of the phases or a scattering of the eccentric particles in the depletion zones. The compression of the streamlines will form the satellite wakes. With the combined effects of collisions and self-gravity, the eccentricity of the wake particles will decrease and the structure will fade. More realistic models involve inter-particle collisions and self-gravity wakes; the latter usually accelerates the damping of the propeller shaped gaps and generally prevents the formation of moonlet wakes.

In our simulations, the boulder stays stable at the center of the simulated box as long as particles are not big enough to change its orbital elements (we verified that this does not happen as long as the particle size radius condition of existence of the depletion zones is respected. It appears that collisions and self-gravity are not playing a key role in the formation of primary propeller signature zones for the initial particle populations described by Zebker et al. (1985) in our regions of interest. However, Lewis & Stewart (2009) showed that self-gravity will generally prevent boulder wakes from forming and will rapidly damp the higher order propeller-shaped gaps. Inputting particles sizes close to the boulder radius will have a similar effect.

We notice that both radial b and azimuthal extensions $r\ \Delta\phi$ of the primary lobe seem to grow linearly with the boulder radius: $b \approx 3\ r_H$, and $r\ \Delta\phi = (33.4 \pm 2.0) r_H$.

3 Results

We identified 35 ghosts in the C ring plateaus and 265 ghosts in the Cassini Division ringlets and plateaus (mainly in the Huygens Ringlet, the Triple Band and the Cassini Division ramp). No real meaningful spatial distribution can be drawn from our observations since we already selected the places where we were observing. However, we notice that ghosts do not appear in similar locations between occultations. We therefore conclude that these features are not complete circular gaps. In addition, we could estimate an observed radial width W for each of the observed ghosts. The ghosts are a few data points wide, and we can estimate their width by taking the width at half-height of the interpolation of the occultation scan. In first approximation, we measured width ranges for the observed ghosts from 5.4 m to 46.7 m in the C ring and from 1.7 m to 277 m in the Cassini Division.

The UVIS instrument has a constant integration time. However, each occultation has a specific navigation and geometry configuration that changes the spatial resolution in the ring plane. The fact that each occultation has its own resolution introduces a bias in our ghost width measures. In order to estimate the impact of this variability and in order to model the difference between the observable widths and the observed widths, we use a Monte Carlo algorithm designed to model the statistical impact of our occultation resolution variations. This algorithm will evaluate the modeled observed ghost widths from a known particle size distribution. We assume that the particle size distribution in the Cassini Division can be modeled as a power-law. From an arbitrary proportion of the total number of particles, we estimate the corresponding particle radius and model the Hill radius of the boulder and then the width of the ghost that would be created. We assume that this ghost is on a random occultation track, at a random azimuthal distance from the boulder (within the range of the primary open gap) and we estimate what would be measured for its width, given the occultation resolution and based on our interpolated model of the ghost width with respect to the distance from the boulder: this observable width can be zero if the resolution of the occultation is larger than the ghost width. The statistical repetition of this process allows us to determine a cumulative size distribution of the theoretically observed ghost widths. By comparing this distribution with the observed ones, we adjust the initial particle size distribution index in order to match the observable distribution with the observed distribution (by matching both the number of the particles and the shape of the distribution). We estimate that a cumulative power-law index of 0.6 in the C ring and 0.8 in the Cassini Division for the initial particle size distribution will generate ghost-width distributions close to the observed ones. This process happens to provide quite close values between the C ring and the Cassini Division. The difference between these indices is of the same order of magnitude as the difference between the distributions of smaller particles by Zebker et al. (1985): $Q_{Cring} = 2.1$ and $Q_{CD} = 1.75$. From these derived indices, we can estimate that the actual boulder population, that generated our observations, follows a cumulative size distribution not in the prolongation of the one for smaller particles.

4 Discussion

In both the C ring and the Cassini Division, we have been able to identify a population of boulders that would be able to create the ghosts we have observed in UVIS occultation data. These boulders follow less steep power-law distributions than smaller particles, and with similar indices between the C ring and the Cassini Division: $0.6 - 0.8$.

Figure 4 compares particle size distributions and boulder size distributions for the C ring and the Cassini Division. Zebker et al. (1985) values for submeter particles were determined with a good accuracy while suprameter particles and in particular upper limits of the distributions were probably overestimated. The boulders appear to not follow the previous trend of the particle size distributions. This is consistent with recent conclusions from Baillié et al. (2011) according to which particles tends to be smaller in the C ring plateaus.

A unique progenitor, big enough to generate the boulder population, would have to be at least 800-m wide for the C ring and at least 2.8-km wide for the Cassini Division. Such small boulders should be able to survive tidal disruption well inside the Roche limit (Goldreich & Tremaine 1982). However, catastrophic disruptions involving cometary collisions would generate a secondary particle population.

In such a scenario, the minor accretion effects would not have allowed the formation of the progenitors in situ. These boulders would have more likely formed outside the main rings and then spiraled inwards by gas drag (Mosqueira & Estrada 2003). They could also be the results of another bigger fragmentation. In addition, we would expect the resulting particle size distribution from a fragmentation process to be steeper than our derived estimations, closer to a power-law distribution with a cumulative index around 3.4 (which is the index obtained for the ejecta of a hammer-destruction of a glacial boulder (Hartmann 1969; Dohnanyi 1969, 1972).

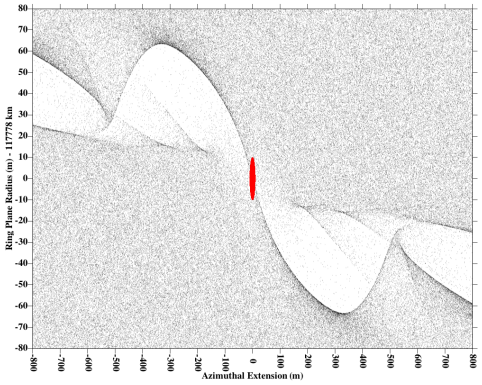

Figure 3. Primary lobes of the propellers created by the interaction of 20-cm radius particles with a 10-m radius boulder. Optical depth is 0.1 and Saturn's direction is towards the bottom.

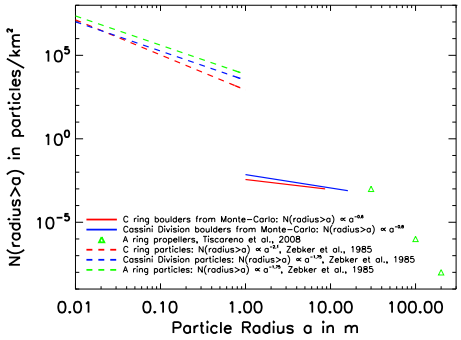

Figure 4. Cumulative particle size distribution for the C ring (red), Cassini Division (blue) and the A ring (green). Submeter particle populations from Zebker et al. (1985) are displayed with dashed lines while the source distribution estimated from the Monte-Carlo algorithm for suprameter particles is displayed in solid lines.

Considering aggregation as the principal effect, it is possible to form temporary aggregates inside the Roche limit (Karjalainen & Salo 2004), which would disturb the encountering particles and clear depletion zones. However, the accretion effects are not predominant in tenuous rings like the C ring or the Cassini Division. In addition, we do not observe any trend in the distribution of our boulder sizes with respect to their distance to Saturn that would strengthen the confidence in this scenario.

This work was supported by NASA through the Cassini Data Analysis Program.

References

Baillié, K., Colwell, J. E., Esposito, L. W., Sremčević, M., & Lissauer, J. J. 2011, Icarus in press
Dohnanyi, J. S. 1969, J. Geophys. Res., 74, 2531
Dohnanyi, J. S. 1972, Icarus, 17, 1
Goldreich, P. & Tremaine, S. 1982, Annual Review of Astronomy and Astrophysics, 20, 249
Hartmann, W. K. 1969, Icarus, 10, 201
Karjalainen, R. & Salo, H. 2004, Icarus, 172, 328
Lewis, M. C. & Stewart, G. R. 2009, Icarus, 199, 387
Mosqueira, I. & Estrada, P. R. 2003, Icarus, 163, 232
Petit, J. & Henon, M. 1988, Astronomy and Astrophysics, 199, 343
Showalter, M. R. & Burns, J. A. 1982, Icarus, 52, 526
Showalter, M. R., Cuzzi, J. N., Marouf, E. A., & Esposito, L. W. 1986, Icarus, 66, 297
Spahn, F., Saar, A., Schmidt, S., & Schwarz, U. 1992, Icarus, 100, 143
Spahn, F. & Wiebicke, H. 1989, Icarus, 77, 124
Sremčević, M., Spahn, F., & Duschl, W. J. 2002, MNRAS, 337, 1139
Zebker, H. A., Marouf, E. A., & Tyler, G. L. 1985, Icarus, 64, 531